Comprehensive approach to tau-lepton production by high-energy tau neutrinos propagating through the Earth

Jaime Alvarez-Muñiz,[1] Washington R. Carvalho, Jr.,[2] Kévin Payet,[3] Andrés Romero-Wolf,[4] Harm Schoorlemmer,[5] and Enrique Zas[1]

[1]*Departamento de Física de Partículas and Instituto Galego de Física de Altas Enerxías, Universidade de Santiago de Compostela, 15782 Santiago de Compostela, Spain*
[2]*Instituto de Física, Universidade de São Paulo, Rua do Matão, 1371 CEP 05508-090 Cidade Universitária, São Paulo, Brazil*
[3]*Université Joseph Fourier (Grenoble I); Currently at La Javaness, 75010 Paris, France*
[4]*Jet Propulsion Laboratory, California Institute of Technology, Pasadena, California 91109, USA*
[5]*Max-Planck-Institut für Kernphysik, 69117 Heidelberg, Germany*

(Received 2 August 2017; published 26 January 2018)

There has been a recent surge in interest in the detection of τ-lepton-induced air showers from detectors at altitude. When a τ neutrino (ν_τ) enters the Earth, it produces τ leptons as a result of nuclear charged-current interactions. In some cases, this process results in a τ lepton exiting the surface of the Earth, which can subsequently decay in the atmosphere and produce an extensive air shower. These upward-going air showers can be detected via fluorescence, optical Cherenkov, or geomagnetic radio emission. Several experiments have been proposed to detect these signals. We present a comprehensive simulation of the production of τ leptons by ν_τ's propagating through Earth to aid the design of future experiments. These simulations for ν_τ's and leptons in the energy range from 10^{15} eV to 10^{21} eV treat the full range of incidence angles from Earth-skimming to diametrically traversing. Propagation of ν_τ's and leptons includes the effects of rock and an ocean or ice layer of various thicknesses. The interaction models include ν_τ regeneration and account for uncertainties in the Standard Model neutrino cross section and in the photonuclear contribution to the τ energy-loss rate.

DOI: 10.1103/PhysRevD.97.023021

I. INTRODUCTION

Despite decades of observation, including currently operating state-of-the-art detectors [1,2], the origin of ultrahigh-energy (UHE, $\gtrsim 10^{18}$ eV) cosmic rays remains unknown, with source model parameters relatively unconstrained [3]. The propagation of UHE cosmic rays through the cosmic photon backgrounds is expected to produce a flux of UHE neutrinos [4–7]. The detection of or tighter limits on this cosmogenic UHE neutrino flux have the potential to significantly constrain models of UHE cosmic-ray sources [8–10].

UHE neutrinos have been searched for in the past decades with several experiments using the Moon [11–13], the Earth's crust with the Pierre Auger Observatory [9], and the Antarctic ice cap with IceCube [10] and ANITA [14], each producing the most constraining limits to date in different parts of the UHE band. Recently an extraterrestrial flux of neutrinos extending above 10^{15} eV has been detected with IceCube [15]. The origin of this flux is unknown and while it is dominated by extragalactic sources [16] it is not expected to be due to the UHE cosmic-ray interaction with cosmic photon backgrounds [17,18]. It is also unknown the extent to which the detected flux can be extrapolated to the UHE band or if there is a cutoff energy [19].

Although cosmogenic neutrinos are expected to be produced predominantly in electron and muon flavors, flavor mixing over cosmic propagation distances predicts a significant fraction ($\sim 1/3$) of τ neutrinos [20,21]. The τ neutrinos (ν_τ) provide a detection channel that is unlike the electron and muon counterparts. When a ν_τ interacts via a charged-current interaction it produces a τ lepton along with a hadronic shower. The τ lepton has an extremely short lifetime compared to the muon, compensating for the enormous Lorentz boost at UHE, so that the τ is likely to decay before losing a significant amount of its energy. One such consequence is the so-called double bang events [21] expected by experiments searching for showers in ice such as IceCube. Another promising channel for detection, where τ leptons produced in the Earth exit into and decay in the atmosphere, producing an up-going extensive air shower, was originally studied in [22,23]. These up-going air showers could be potentially observed by the surface detector of the Pierre Auger Observatory [9] as an Earth-skimming shower [24,25], and they are potentially observable from a high-altitude observatory such as ANITA [26].

Recently, several experiments have been proposed to search for this signal such as Ashra [27] and CHANT [28] using optical Cherenkov detection and GRAND [29] using a ground array of radio detectors.

The propagation of ν_τ's entering the Earth resulting in a τ lepton exiting into the atmosphere is a complex problem involving multiple scales. It involves the combined effect of the τ-lepton lifetime, its energy loss, and the neutrino cross section, each having a different dependence on energy, together with the available matter depth, which is a rapidly varying function of the ν_τ incidence angle (see, for instance, [30] for a review). As the neutrino propagates through the Earth, the ν_τ flux is attenuated because of interactions. However, there is also a "regeneration" effect [31,32]: charged-current interactions followed by τ-lepton decays (in which a lower-energy ν_τ is always produced), as well as neutral-current interactions, shift down the neutrino energy, "regenerating" the ν_τ flux. The effect of regeneration depends heavily on the ν_τ incidence angle. It can be negligible for Earth-skimming trajectories but result in well over a factor of two shift in ν_τ energy for incidence angles with higher depth. In addition, it has been shown that because of the competition between energy loss and decay, the density of the matter just before the τ lepton exits the Earth can have a significant impact on the rate of exiting τ leptons, which is important for observation near the ocean or the ice caps [33].

The τ-production mechanism also depends crucially on uncertainties on the neutrino-nucleon cross section as well as the τ-lepton energy-loss rate at UHE, both of which have to be extrapolated to kinematical regions which are well outside those that have been explored in accelerators. Several publications have studied the propagation and detectability of τ leptons exiting the Earth into the atmosphere in different energy and angular ranges [32–44]. These studies use Monte Carlo simulations and/or semianalytical techniques to estimate the sensitivity for detectors underwater or in ice as well as ground-level arrays of particle and fluorescence detectors.

The objective of the comprehensive simulations presented in this paper is to provide useful results for the design of future detectors including the effects that are relevant to observations over rock, ocean, or ice from the ground or at altitude, while considering uncertainties in the interaction models. We present the characteristics and results obtained with a simulation based on [45] for estimating the probability and energy distribution of τ leptons exiting the surface of the Earth given a UHE ν_τ flux entering at a given incidence angle. The simulation accounts for the particle interactions, energy loss, and decay processes relevant to the propagation of ν_τ's through the Earth, including ν_τ regeneration, as well as for the geometry of the propagation, including the features of the Earth density profile (with spherical symmetry), and adjustable ocean/ice layer thickness, all in a single simulation package.

The simulation can be used in a wide energy and angular range relevant for most experiments, namely, from 10^{15} eV to 10^{21} eV in ν_τ energy and the full incidence angle range $0° - 90°$. A recent study [44] produced simulations with detailed models of neutrino interaction cross sections and τ-lepton energy-loss models with a consistent account of inelasticity. The simulations presented here also allow for variations of the cross-section and energy-loss model, although in a less detailed manner (see Sec. III). However, we also include the effects of a layer of ice or water as well as regeneration, which were not included in [44]. While these effects may not be relevant to estimating the sensitivity of the Pierre Auger Observatory (as done in [44]), they may be relevant to interpreting τ-lepton air showers observed at altitude, as mentioned in [26].

The simulation package used to produce the results of this paper is being made publicly available.[1] The simulation allows the user to specify functions for neutrino-nucleon and photonuclear contributions to tau energy-loss curves that account for Standard Model uncertainties. The executable takes in the incident ν_τ energy, direction, number of injected neutrinos, cross section, and energy-loss model in the command line, and it produces a list of τ-lepton energies that exit into the atmosphere. A novel feature of the simulation is that it tracks the chain of ν_τ interactions and τ lepton decays that lead to the production of an exiting τ lepton, shedding light on their production mechanism as a function of incidence angle and the initial ν_τ energy. The simulation has been designed with the intention that other models, a more detailed accounting of particle interactions, or additional media effects may be easily included for future developments.

The paper is organized as follows. In Sec. II we provide a summary of ν_τ propagation through the Earth. In Sec. III we review some of the Standard Model uncertainties in the neutrino-nucleon cross section and τ-lepton energy-loss rate. In Sec. IV we give results for the dependence of the exiting τ lepton flux on ν_τ energy, ν_τ regeneration, ice layer thickness, and particle interaction models. In Sec. V we provide a discussion of the results and conclusions.

II. TAU NEUTRINO PROPAGATION THROUGH THE EARTH

As a ν_τ of energy E_ν propagates through the Earth, it will primarily interact with nucleons, which can result in the production of a τ lepton. The processes involved in ν_τ and τ-lepton propagation are shown in Fig. 1. A neutral-current (NC) interaction occurs ~28% of the time, resulting in the production of a hadronic shower and a ν_τ. The secondary ν_τ carries a fraction of the energy given by $(1 - y)E_\nu$. The lab-frame inelasticity y is a standard dimensionless variable corresponding to the fraction of the neutrino energy carried away by the hadronic shower. The y distribution is noncentralized with an average $\langle y \rangle \simeq 0.2$ at UHE [46] and

[1] https://github.com/harmscho/NuTauSim

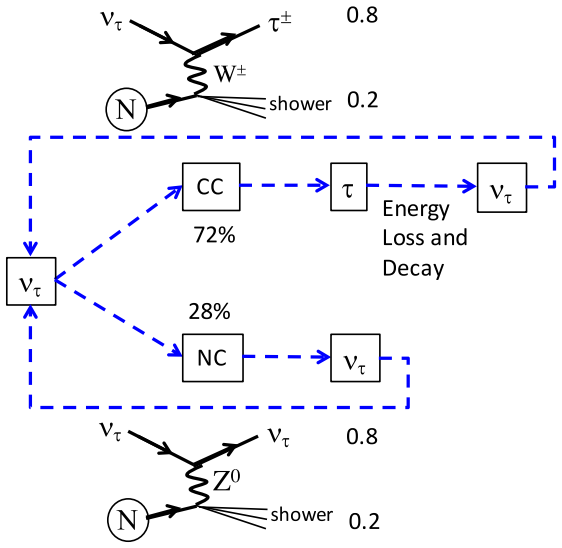

FIG. 1. Diagram of the ν_τ propagation process. A ν_τ can interact either via charged-current (CC) or neutral-current (NC) interaction. The CC interaction occurs ~72% of the time and results in the production of a τ lepton, carrying on average ≃80% of the energy of the ν_τ at UHE and loses energy while propagates. The τ lepton can escape the Earth before it decays. If it decays in the Earth, it will produce a ν_τ, which will continue to propagate. NC interactions occur ~28% of the time and produce a ν_τ which also continues to propagate. See text for more details.

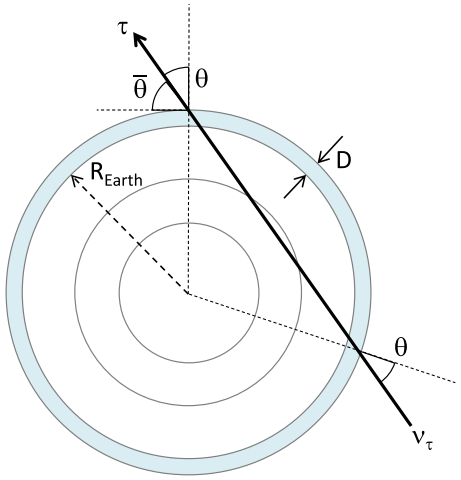

FIG. 2. Simulation geometry for a ν_τ entering the Earth with incidence angle θ. The model of the Earth assumes a sphere of radius $R_{\rm Earth}$ and adjustable ocean or ice depth D. The ν_τ is injected with a specified exit angle θ, which determines the trajectory it will take across the various subsurface layers of varying density where the interactions will take place. Results are given in terms of the emergence angle $\bar{\theta} = 90° - \theta$, which is the complement of the exit and entry angles.

large variance. The hadronic shower energy is absorbed in a few tens of meters in the Earth, while the ν_τ continues to propagate. A charged-current interaction (CC) occurs ~72% of the time, producing a hadronic shower and a τ lepton. The average fraction of the energy carried away by the hadronic shower at UHE is also $\simeq 0.2E_\nu$ with a similar y distribution.

As the produced τ lepton propagates through the Earth, it will lose energy via ionization, pair-production, and photonuclear interactions. The τ lepton will decay with a lifetime of 0.29 ps in its rest frame, which, for a given energy E_τ, corresponds to a *decay length* of $(E_\tau/10^{17}\ \text{eV}) \times 4.9$ km. At low energies the τ lepton tends to decay before losing a significant amount of energy, and the τ range increases linearly with energy because of the Lorentz boost. However, this behavior changes above an energy scale typically in the range between 10^{17} eV and 10^{18} eV [30]. In this regime energy losses decrease the τ-lepton energy until it either decays or exits the Earth, depending on the available matter depth. If the τ lepton decays inside the Earth, it produces a variety of particles, depending on the decay mode, always including a regenerated ν_τ with lower energy that continues to propagate.

When the τ lepton exits the Earth's crust into the ~1000-times-lower-density atmosphere, it undergoes negligible energy loss. The dominating process in this case is τ decay, described by an exponentially falling distribution characterized by the decay length. The decay products result in hadrons >60% of the time or in an electron with a branching ratio of 17.9%. In both cases an extensive air shower is produced provided the decay happens in the atmosphere. The decay can also result in a muon 17.9% of the time, which is unlikely to result in an extensive air shower. The τ lepton decays in the atmosphere and their subsequent air showers are not handled by the Monte Carlo simulations presented here.

The relevant geometric parameters of the simulation are shown in the diagram in Fig. 2. The direction of the injected neutrino is determined by the incidence angle θ. For our spherically symmetric model, the exit angle is identical to the incidence angle. The complement is the emergence angle $\bar{\theta} = 90° - \theta$. The Earth is modeled as a sphere of radius $R_{\rm Earth}$ with subsurface layers of varying density according to the Preliminary Earth Reference Model [47]. An ocean or ice layer of thickness D can be specified in the simulation.

The interactions of the injected particle are randomly sampled while it propagates. The depth traversed by the ν_τ before interacting is obtained from an exponential distribution with mean free path determined by the total cross section as a function of E_ν. Whether the interaction is CC or NC is randomly chosen according to their relative weight on the total cross section (CC/NC ≃ 2.6/1 at UHE). In the case of a NC interaction, the ν_τ propagation proceeds with the new value of E_ν sampled from the y distribution. In the case of a CC interaction, the energy of the resulting τ lepton is also sampled from the same y distribution. The τ-lepton propagation accounts for energy loss in small depth steps and at each step the probability of decay is evaluated at the new τ lepton energy and randomly sampled from an

exponential distribution. If the τ lepton decays, the energy of the resulting ν_τ is sampled from the corresponding distribution obtained with the TAUOLA package [48] with an average value of $\langle E_\nu \rangle \simeq 0.3 E_\tau$. The simulation stops when either the propagating ν_τ or τ lepton exits the Earth into the atmosphere. In the case of an exiting τ lepton, the simulation records its final energy, emergence angle, the initial ν_τ energy, the number of CC interactions (at least one), NC interactions, and τ lepton decays (if any). This feature of the simulation allows us to study in detail the chain of events that typically lead to the production of τ leptons in the atmosphere as a function of the initial ν_τ energy E_ν and emergence angle $\bar{\theta}$.

III. NEUTRINO INTERACTION AND TAU ENERGY-LOSS MODELS

The main source of uncertainty in the calculation of the τ-lepton fluxes arises because the neutrino cross section and the τ energy loss are needed in an energy range where there are no experimental data. Neutrino cross sections and τ energy losses are calculated using the Standard Model and require extrapolating the structure functions of the nucleons to kinematical regions that are unexplored. Structure functions depend on the four-momentum of the nucleon p and the four-momentum transferred to the nucleon q, but they are typically described in terms of the two independent variables $Q^2 = -q^2$ and $x = Q^2/(2p \cdot q)$. The kinematical region mostly contributing to the neutrino cross section and τ-lepton energy losses are different. While in both regions the relevant values of x are extremely low, for the neutrino cross section $Q^2 \sim M_W^2 \sim 6400$ GeV^2, of order the mass squared of the exchanged weak bosons, while for the τ-lepton energy loss Q^2 is between $\sim$1 and 100 GeV^2 [49]. The two regions cannot be described by a single formalism. Different approximations and extrapolations are needed in each case.

Standard Model uncertainties in the neutrino-nucleon cross section can be quite large, reaching up to a factor of five at energies of 10^{21} eV, according to [50]. It is not the purpose of this work to explore these uncertainties. We have considered characteristic cross sections as given in [50] (see Fig. 3 and Table I). We have chosen to include the central value of the cross section together with the given parametrizations of the upper and lower limits of the uncertainty band as options. They give us an order of magnitude estimate of the uncertainties involved within the Standard Model. We note that alternative calculations based on the dipole model [44] can give even slightly lower values (order 20%) at 10^{18} eV. Moreover there have been several studies on new physics that could suppress or enhance the cross sections at high energies well beyond the chosen uncertainty band (see, for instance, [51–53]).

For this study, we have not considered the uncertainties in the y distributions and we use the results from standard calculations using parton distributions [54] throughout. The

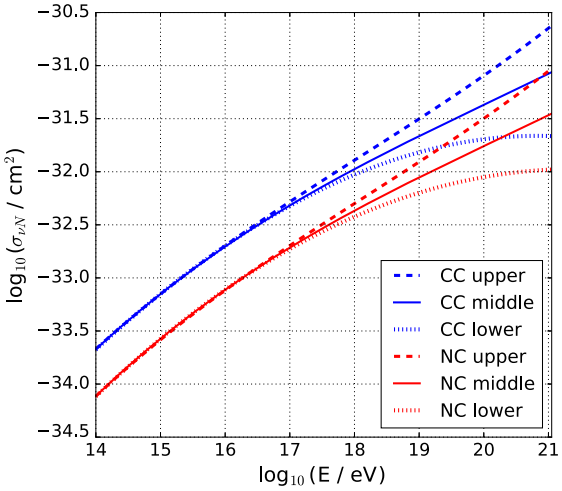

FIG. 3. Standard Model charged-current (CC) and neutral-current (NC) neutrino-nucleon cross sections $\sigma_{\nu N}$ as a function of energy from [50]. The upper and lower curves represent the upper and lower limits of the uncertainties due to the parton distribution function. In this work we consider the upper, middle, and lower curves in the calculation of the probability and energy distribution of exiting τ leptons.

work of [44] included the full dependence on the y distribution and the authors concluded that the results can be reproduced accurately using only the average $\langle y \rangle$ as a function of energy. Between the models considered in [44], changes in $\langle y \rangle$ range from -3% to 7% at 10^{15} eV and -15% to 23% at 10^{20} eV. The resulting fluxes in that reference show consistent results with different models within 25%. If the logarithmic slope of the structure functions is significantly altered from the values obtained from extrapolating the parton distributions, the average value of y can change [55]. Dependence on the y distribution is not addressed further in this article. Alternative parametrized cross sections or y distributions could be readily included in the simulation code to produce results for the τ-lepton exit probability and energy distribution as a function of exit angle.

The τ-lepton energy-loss rate is often parametrized as

$$\left\langle \frac{dE_\tau}{dx} \right\rangle = -a(E_\tau) - b(E_\tau) E_\tau, \tag{1}$$

TABLE I. Parameters for the log-log polynomial fit $\log_{10}(\sigma/\mathrm{cm}^2) = \sum_{k=0}^{3} p_k (\log_{10}(E/\mathrm{eV}))^k$ to the Standard Model neutrino cross sections (see Fig. 3).

Cross section	p_0	p_1	p_2	p_3
CC upper	−53.1	2.73	−0.129	0.00237
CC middle	−53.5	2.66	−0.114	0.00182
CC lower	−42.6	0.49	0.003	−0.00133
NC upper	−53.7	2.73	−0.127	0.00231
NC middle	−54.1	2.65	−0.112	0.00175
NC lower	−44.2	0.71	0.002	−0.00102

where a and b are slowly varying functions of the τ-lepton energy. The parameter a accounts for ionization processes and is practically constant $a \approx 2 \times 10^6$ eV cm^2/g at energies much larger than the τ-lepton mass relevant to this work. The parameter $b(E_\tau)$ includes contributions from bremsstrahlung, pair-production, and photonuclear interactions. At energies $E_\tau > 10^{16}$ eV, photonuclear interactions have the largest and most uncertain contribution to b, which is also due to uncertainties in the knowledge of the parton distribution functions in the corresponding kinematic region (see, for instance, [44,49]).

We again consider parametrizations of two models of the contribution of the photonuclear interaction to the energy-loss rate: ALLM [56] and ASW [57]. The fractional energy-loss rate for each model is shown in Fig. 4. For the purposes of this study, we take ALLM to be a typical model, while ASW represents a model with suppressed photonuclear energy-loss rate. The parametrizations are given by a power law in energy $b(E_\tau) = p_0 + p_1(E_\tau/\mathrm{GeV})^{p_2}$ with parameters provided in Table II. In contrast to [33], we use the same results for water and rock when the depth x is expressed in g cm^{-2} since differences due to nuclear effects are relatively insignificant compared to other uncertainties.

The neutrino-nucleon cross section and the photonuclear contribution to the τ-lepton energy-loss rate are calculated from extrapolated structure functions. We take the uncertainties in both processes to be independent (see, however, [44]). This approach is justified since the ranges of the kinematical variables (Q^2 and Bjorken-x) that contribute to the neutrino cross section (dominated by perturbative QCD) and τ-lepton energy loss (where perturbative and nonperturbative effects are mixed) are quite different at 10^{18} eV energies, and none of the available parametrizations of the parton distributions is adequate to describe both ranges simultaneously [49].

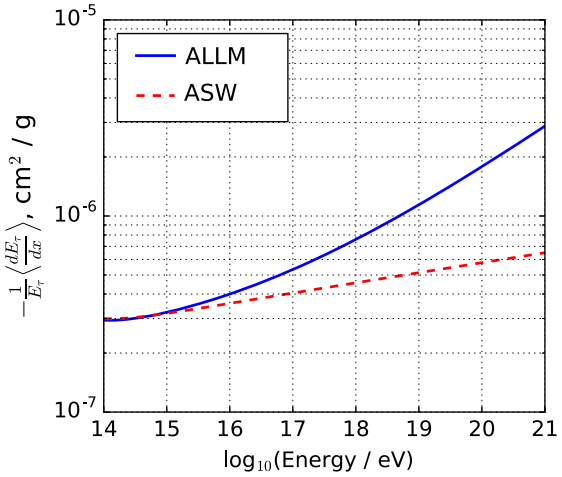

FIG. 4. Fractional τ-lepton energy-loss rate $\frac{1}{E_\tau}\langle\frac{dE_\tau}{dx}\rangle$, including ionization, pair production, bremsstrahlung, and photonuclear interactions as a function of energy. The two curves shown are for the ALLM [56] and ASW [57] photonuclear interaction models.

TABLE II. Parameters for the power law fit to the $b(E_\tau)$ function of the energy-loss rate in Eq. (1) (see Fig. 4). The parametrization is $b(E_\tau) = p_0 + p_1(E_\tau/\mathrm{GeV})^{p_2}$.

$b(E_\tau)$	p_0 (cm^2/g)	p_1 (cm^2/g)	p_2
ALLM	2.06×10^{-7}	4.93×10^{-9}	0.228
ASW	-4.77×10^{-7}	1.90×10^{-7}	0.047

IV. RESULTS

The simulation presented here allows for variations in the emergence angle $\bar{\theta}$, incident neutrino energy E_ν, thickness D, and density of the water layer, together with the cross section and energy-loss models as described above. The number of combinations is far too great for a comprehensive study. Instead, we will narrow down some comparisons that characterize the dependence on these variables.

A. Tau lepton production dependence on neutrino energy

We characterize the behavior of various injected neutrino energies while taking the cross sections corresponding to the middle curves and the ALLM energy-loss rate model. We treat the case of a $D = 4$ km thick layer of ice, corresponding to the thickest regions of the Antarctic ice sheet. This is quite similar to what can be expected for an average ocean depth of (~3.7 km) given that the density of ocean water is ~10% greater than ice.

If a ν_τ enters the Earth either a τ lepton or a ν_τ must exit at the other side because the τ lepton always decays into a ν_τ even if the energy of the exiting lepton can be significantly reduced. For the τ lepton to be injected into the atmosphere, the CC interaction must happen before the exit point and within the tau range. The closer it happens to the exit point, the higher the tau energy at injection. The effective interaction volume for neutrino interactions is adjacent to the Earth's surface and scales with the τ-lepton range.

In Fig. 5 we show the probability that a τ lepton exits the volume of the Earth (P_{exit}) given an injected ν_τ of energy E_ν. The probability is highest for large E_ν in Earth-skimming trajectories at small emergence angles ($\bar{\theta} < 2°$). The feature at $\bar{\theta} = 2°$ corresponds to the direction of propagation that is tangential to the layer of rock beneath the $D = 4$ km thick ice layer (see Fig. 2). For lower E_ν, when the ν_τ interaction cross section is reduced, P_{exit} is typically smaller and the curves in Fig. 5 broaden and have fewer features.

The emerging τ-lepton energy E_τ has a distribution which depends on the emergence angle and on the primary neutrino energy in a complex way as shown in Fig. 6. In each panel we show the mode of the E_τ distribution along with the densest ranges containing 68% and 95% of the distribution as dark-gray and light-gray areas, respectively. In Fig. 7 we also show the mean number of ν_τ CC and NC interactions as well as the mean number of τ-lepton decays

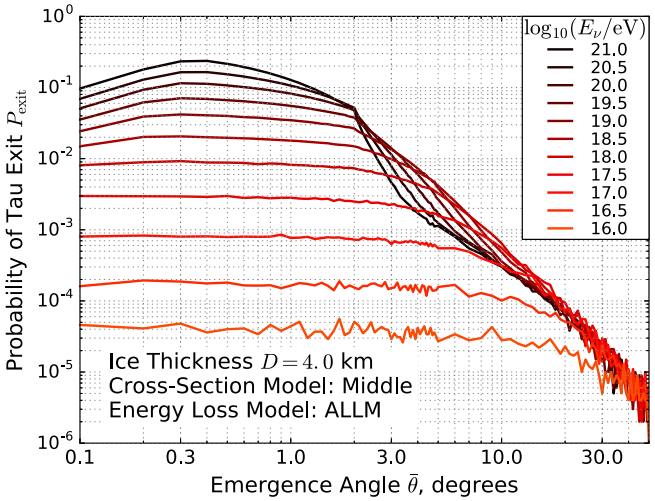

FIG. 5. The probability $P_{\rm exit}$ that a τ lepton exits the Earth's surface for emergence angles between 0.1° (Earth skimming) and 50° given a 4 km thick layer of ice with the standard cross section and energy-loss models. The feature at the emergence angle of 2° corresponds to the trajectory tangential to the rock layer beneath the 4 km thick layer of ice.

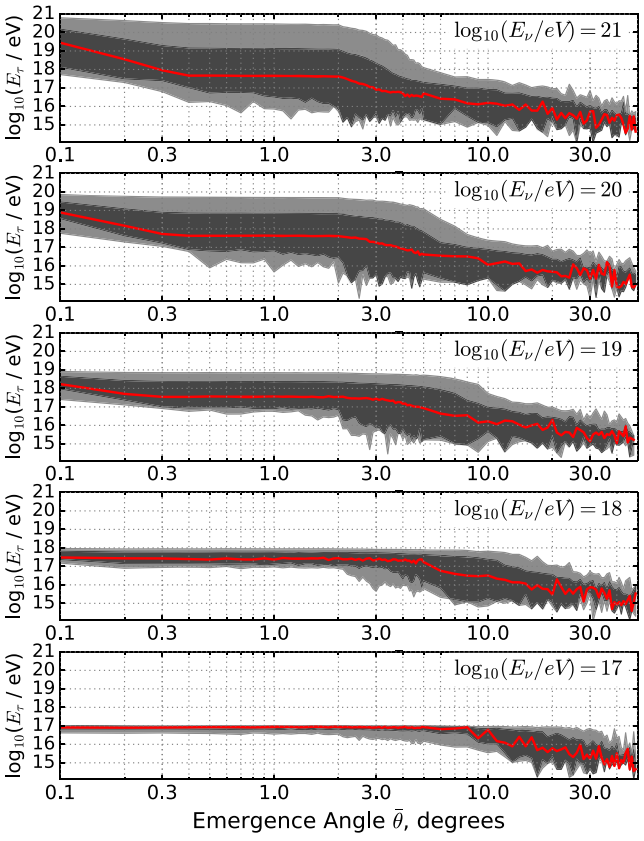

FIG. 6. The exiting τ lepton energies corresponding to some of the energies shown in Fig. 5. The red line shows the most probable exiting tau lepton energy. The dark (light) gray band shows the 68% (95%) densest probability interval. The features in the curves are caused by regions where various interaction processes dominate. See Fig. 7 and text for details.

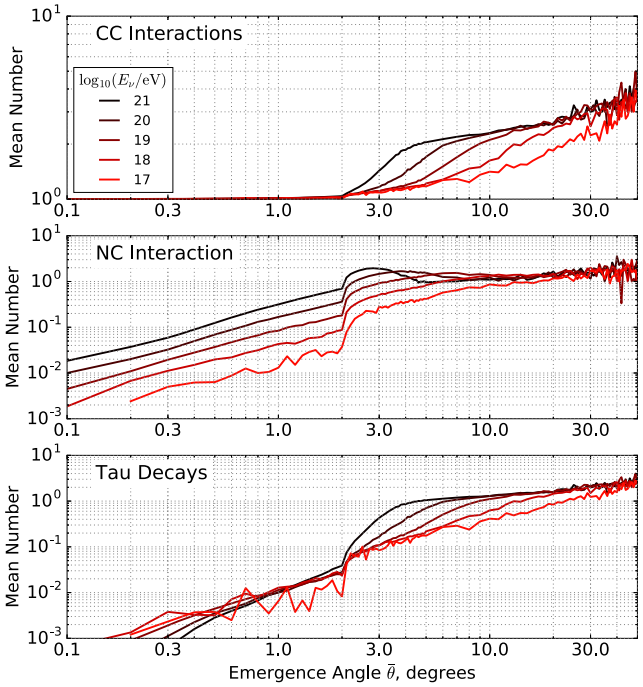

FIG. 7. The mean number of CC, NC interactions, and tau lepton decays as a function of emergence angle for various incident neutrino energies corresponding to Figs. 5 and 6. Top panel: The mean number of CC interactions must be at least 1 since we are selecting particles resulting in a τ lepton exiting the Earth's surface. Middle panel: The mean number of neutral-current interactions. The sharp transition at emergence angle $\bar{\theta} = 2°$ corresponds to the direction tangential to the subsurface rock beneath a 4 km thick layer of ice. Bottom panel: The mean number of τ lepton decays also show a feature at $\bar{\theta} = 2°$. Note that for $\bar{\theta} < 2°$ the particle traverses ice only, while for $\bar{\theta} > 2°$ the particle traverses a combination of rock and ice, which affects the behavior of the τ-lepton and ν_τ interactions.

as a function of $\bar{\theta}$ for selected neutrino energies, to better characterize the features in Fig. 6.

The behavior of the conversion probabilities to exiting τ leptons and the corresponding E_τ distributions can be understood in terms of three scales. The length of the Earth's chord is linearly dependent on $\sin\bar{\theta}$, being 24 km (240 km) for 0.1° (1°). Its column density scales with length up to $\bar{\theta} \simeq 2°$, where there is a discontinuity tangent to the bedrock. Its length is relevant in relation to the τ-lepton decay, while its grammage governs neutrino interactions and τ-lepton energy loss. A second scale is the interaction depth for the neutrino conversion to a τ lepton, which decreases as the neutrino energy rises. For the reference cross section it corresponds to an interaction length of about 1800 km in ice for 10^{18} eV neutrinos and decreases by about a factor of two per decade becoming about 225 km of ice for 10^{21} eV. As long as the interaction depth is much greater than that of the chord, we can expect a single CC interaction and negligible effects to the neutrino flux because of attenuation or regeneration. The third scale is

given by the τ-lepton range. At low energies it scales with the τ-lepton energy, but when the energy exceeds a critical value, $E_{\rm crit}$, the τ-lepton range is determined by energy loss and can be shown to scale roughly as $\log(E_\tau/E_{\rm crit})/b(E_\tau)$. In this regime the τ lepton loses energy rapidly until it approaches $\sim E_{\rm crit}$ when decay quickly follows. If $b(E_\tau)$ and the target density ρ are constant, $E_{\rm crit} \sim m_\tau c^2/(\rho c \tau_\tau b)$, where m_τ and τ_τ are the rest mass and lifetime of the τ lepton [30]. The dependence on ρ is responsible for some of the differences between ice and rock targets. For $\rho = 0.925$ g cm^{-2} and $b \sim 6.5 \times 10^{-7}$ g cm^{-2} its value is $E_{\rm crit} \sim 3.4 \times 10^{17}$ eV.

We can see a distinct behavior of the E_τ distributions in different $\bar{\theta}$ ranges. The transition points depend on the neutrino energy. We consider two broad cases in relation to neutrino energy:

(1) For $E_\nu \gtrsim 3 \times 10^{18}$ eV the trajectory undergoes, on average, a single CC interaction up to about 2°, as seen in Fig. 7, and the τ lepton can lose a large fraction of its energy before exiting. For increasing $\bar{\theta}$, the trajectory has higher interaction probability and more τ-lepton energy loss on average (see Fig. 6) and as a result the mode of E_τ drops and its variance increases. The conversion probability peaks when the Earth's chord roughly matches the tau range at $\sim$0.4° ($\sim$0.2°) for $E_\nu = 10^{21}$ (10^{19}) eV. At larger $\bar{\theta}$ the neutrino can interact early in the chord so that the τ lepton decays before exiting, decreasing the conversion probability.

The mode of the E_τ distribution has a roughly exponential decrease as $\bar{\theta}$ increases until it reaches a plateau when the chord matches the τ-lepton range (see Fig. 6). In the plateau the increase of grammage as $\bar{\theta}$ rises hardly alters the exiting τ-lepton energy distribution, the relevant condition being that the interaction is produced within the τ-lepton range of the exiting point. The average emerging τ-lepton energy is roughly $\sim E_{\rm crit}$ in the plateau for all neutrino energies since this is the energy at which the tau preferentially decays. The plateau ends when the Earth's chord reaches a grammage that attenuates the incident neutrino flux. For larger $\bar{\theta}$, regeneration becomes quite important as can be seen in Fig. 7.

(2) For lower neutrino energies, $E_\nu \leq 3 \times 10^{18}$ eV, the characteristics are similar but the transitions occur at very different values of $\bar{\theta}$. The increase in the conversion probability as $\bar{\theta}$ rises happens at extremely low angles that can hardly be noticed in the plots shown because the τ-lepton range is very much reduced. The plateau reaches larger values of $\bar{\theta}$ because attenuation and regeneration of the neutrino flux require more matter depth.

The relatively large variance of E_τ at high neutrino energies and low $\bar{\theta}$ is largely due to the fact that the neutrino CC interaction can occur anywhere in the trajectory. The upper end of the E_τ distribution is constrained by the neutrino energy and the lower tail by energy loss and decay of the τ lepton. As the neutrino energy drops, the variance of the E_τ distribution decreases. At low incident neutrino energies, the tau energy loss is relatively small because decay dominates. On the other hand, when $\bar{\theta}$ is sufficiently large for regeneration to become important, the width of the E_τ distribution becomes again relatively wide because of the fluctuations inherent to the regeneration processes.

B. Dependence on regeneration

To illustrate the magnitude and importance of the effect of including the ν_τ regeneration, we compare simulation results with regeneration deactivated. In Fig. 8 we show the τ-lepton exit probability as a function of the emergence angle with and without regeneration. In the absence of regeneration, the exit probability is clearly suppressed for emergence angles $\bar{\theta} > 2°$, corresponding to the exit angles where the particle traverses rock as opposed to pure ice. With increasing emergence angles, ignoring ν_τ regeneration underestimates the τ-lepton exit probability by orders of magnitude.

The τ-lepton exit energy distributions for injected neutrino energy of $E_\nu = 10^{20}$ eV with and without regeneration are shown in Fig. 9. Neglecting ν_τ regeneration is consistent with regeneration while $\bar{\theta} < 0.4°$. In the range $0.4° < \bar{\theta} < 3°$ the most probable values are similar;

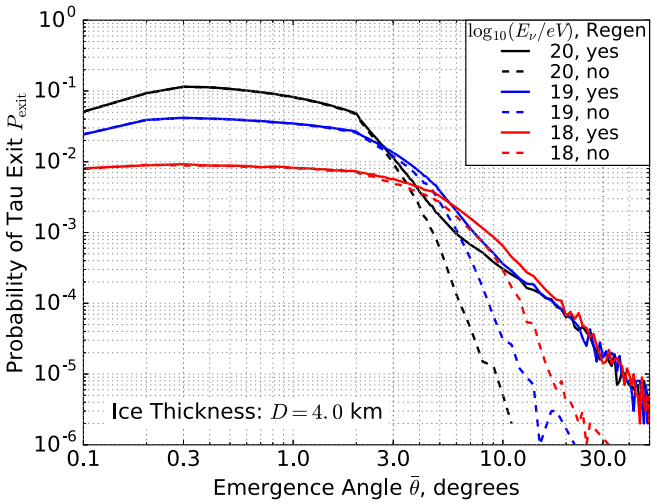

FIG. 8. The probability that a τ lepton exits Earth's surface including and excluding the effect of ν_τ regeneration given a 4 km thick layer of ice and standard neutrino cross section and tau-lepton energy-loss models. Excluding regeneration significantly underestimates the probability of exiting τ leptons for $\bar{\theta} > 2°$, where the trajectories propagate through rock rather than pure ice.

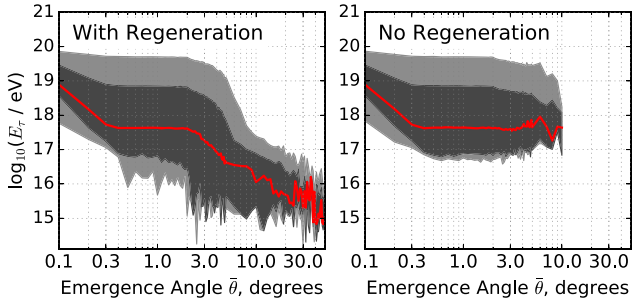

FIG. 9. The exiting τ-lepton energies corresponding to $E_\nu = 10^{20}$ eV in Fig. 8 with and without regeneration. Excluding regeneration suppresses exiting τ leptons with energy $E_\tau < 10^{17}$ eV.

however, the low-energy tail of the E_τ distribution is missing in this approximation. For $\bar{\theta} > 3°$ the energy distributions vary significantly. This is to be expected given that the number of τ-lepton decays becomes significant in this range as shown in Fig. 7. At $\bar{\theta} > 10°$ the distribution is not shown in Fig. 9 due to a lack of events.

C. Dependence on ice layer thickness

The presence of a layer of ice or water can be an important consideration for the design of experiments. In Fig. 10 we show the dependence of P_{exit} on the ice thickness for several neutrino energies between 10^{17} and 10^{20} eV. For energies $>10^{18}$ eV, there is a stark difference between bare rock and the presence of a layer of ice, even if the ice is just 1 km thick. For each thickness, a break in the curve is found at the angle corresponding to the direction of propagation that is tangential to the layer of rock beneath the ice (1°, 1.4°, 1.8°, 2.0° for 1, 2, 3, and 4 km ice thickness, respectively). For $\bar{\theta}$ around the angle at which this feature occurs, the exit probability can be close to a factor of five greater than bare rock at $E_\nu = 10^{20}$ eV, in qualitative agreement with the results of [33]. At neutrino energies $E_\nu < 10^{18}$ eV, bare rock has an advantage over the presence of a layer of ice. For $E_\nu = 10^{17}$ eV, bare rock has roughly twice the P_{exit} than cases with an ice layer for emergence angles $\bar{\theta} < 3°$.

The effect is not intuitive because the relative probabilities that a τ lepton exits the atmosphere depend on neutrino energy. The results for neutrino energies of 10^{19} eV and 10^{20} eV shown in Fig. 10 are characterized by the τ lepton being above the critical energy E_{crit} described in Sec. IV A, while 10^{17} eV and 10^{18} eV are below it. E_{crit} effectively separates the energy into high- and low-energy regions in which the τ-lepton range is respectively governed by energy loss or decay. For neutrino energies 10^{19} eV and 10^{20} eV, the τ-lepton range is dominated by energy loss while for 10^{17} eV and 10^{18} eV, the range is dominated by decay lifetime.

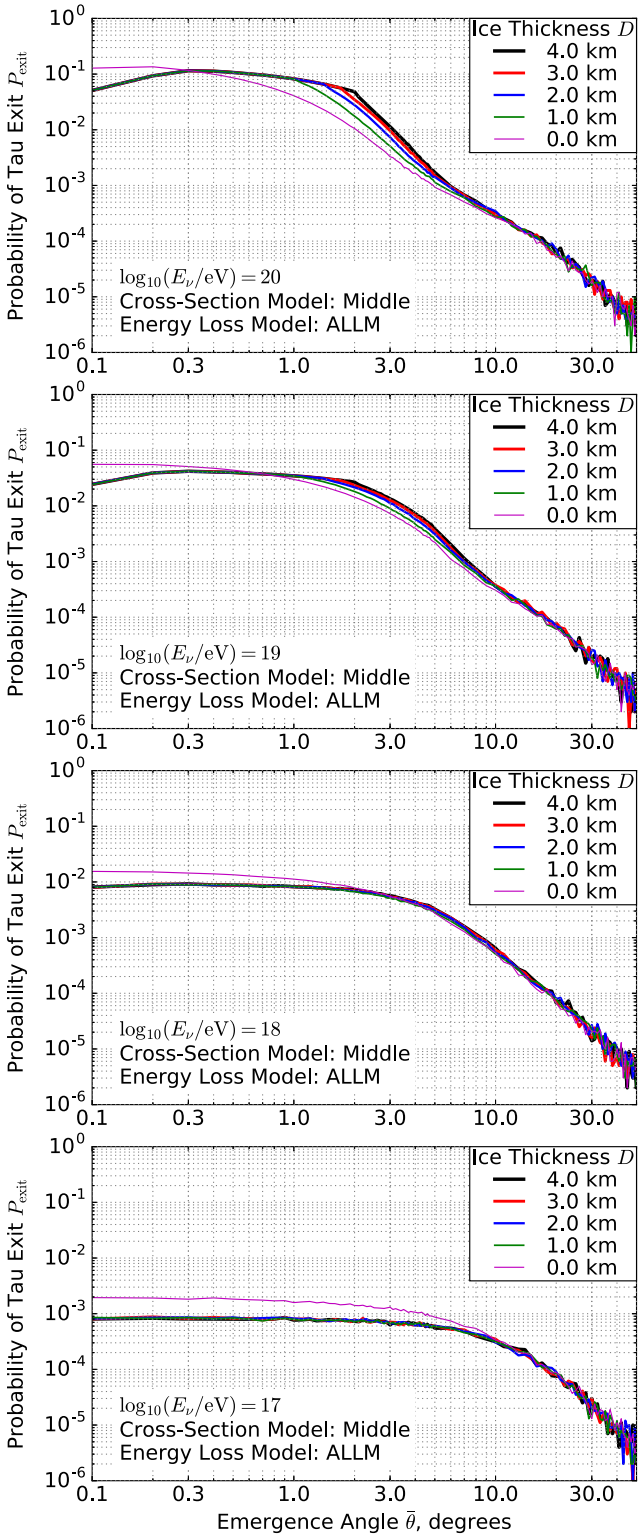

FIG. 10. The probability that a τ lepton exits the Earth's surface for various energies and ice thicknesses, including bare rock, assuming standard cross section and energy-loss models. From top to bottom, the input neutrino energies are 10^{20}, 10^{19}, 10^{18}, and 10^{17} eV. A layer of ice is favorable to exiting τ leptons for neutrino energies $>10^{18}$ eV, while bare rock is favorable for neutrino energies $<10^{18}$ eV. See text for details.

In the 10^{20} eV regime, the τ-lepton range is of order 60 km in ice and 25 km in rock for the ALLM model. If the chord length is larger than this range, the region where the τ can exit efficiently will be proportional to the τ range and independent of the chord length. This can be seen in Fig. 10 for rock at $E_\nu = 10^{20}$ eV above 0.1° (22 km of chord length) and below ~0.2°. In this small angular range and for this energy, the larger interaction probability of ν_τ in rock makes the exiting probability larger than in ice. However, at this same energy and for $\bar{\theta} > 0.3°$, where the range in rock is smaller than the chord, the lower density of ice reduces the τ-lepton energy loss, and as a consequence the τ-lepton range and hence the exit probability are larger. As the emergence angle $\bar{\theta}$ (and chord length) increases, the chord (150 km at 0.7° for 10^{20} eV) becomes comparable to the neutrino interaction length and attenuation sets in suppressing the exit probability.

In the 10^{17} eV regime, on the other hand, the τ-lepton range is of order 5 km. At this energy regime, there is no significant difference in decay range for rock and ice because energy loss (and therefore the density) is not a significant effect. However, the higher density of rock increases the probability that a ν_τ will interact near the surface compared to ice, which explains the higher value of P_{exit} in the bottom graph of Fig. 10.

At high energies (10^{19} eV and above), the curves show a discontinuity when the trajectory is tangent to the rock surface above which neutrino attenuation in the rock takes over, while at low energies there is no discontinuity. This effect is also dependent on whether the τ-lepton range is dominated by energy loss or decay lifetime since the former is sensitive to the density of the medium while the latter is not.

Finally, there is a change of behavior when regeneration takes over at angles of order $\bar{\theta} > 3°$ for $E_\nu = 10^{20}$ eV and $\bar{\theta} > 10°$ for $E_\nu = 10^{17}$ eV. In this regime the relative change in grammage for the two cases is small, and the curves for rock and ice become very similar.

As a general conclusion, the increased P_{exit} and exiting E_τ indicates that the presence of an ice or water layer is highly favorable for detection at energies $E_\nu > 10^{18}$ eV, while bare rock is more favorable for $E_\nu < 10^{18}$ eV.

D. Model dependence

We have considered different neutrino cross-section models consistent with the uncertainties in the Standard Model and a couple of τ-lepton energy-loss-rate models to illustrate the effect of suppression. In Fig. 11 we show the P_{exit} curves corresponding to combinations of these models. The effect of reducing the cross section is that P_{exit} decreases below an emergence angle that coincides with the direction tangential to the bedrock ($\bar{\theta}_C \sim 2°$), for the chosen ice layer depth of 4 km, while it increases at larger emergence angles. This is because for low grammage

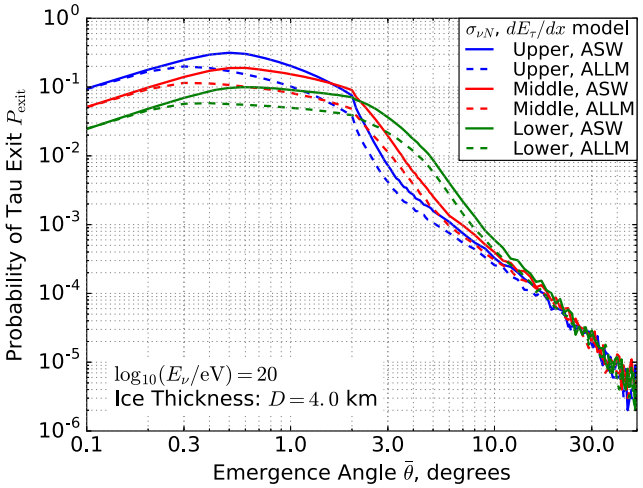

FIG. 11. The probability that a τ lepton exits the Earth's surface for various combinations of neutrino cross section and τ-lepton energy-loss models given a 4 km thick ice layer for a 10^{20} eV injected ν_τ. Lowering the cross section has the general effect of reducing the τ lepton exit probability for emergence angles below where the trajectory is tangential to the subsurface rock layer while increasing the probability for larger emergence angles. The ASW energy-loss-rate model, which is suppressed compared to the more standard ALLM model, results in an overall increase in τ lepton exit probability.

the interaction probability drops, while in the high grammage region the attenuation of the ν_τ flux is reduced for a smaller cross section. The values of P_{exit} are higher for the saturated ASW model with lower energy loss than for the more standard ALLM model. Differences can reach up to a factor of ten in the region of $\bar{\theta} \sim 4° - 5°$.

All curves converge for emergence angles $\bar{\theta} > 20°$ where the effect of regeneration is strongest. Regeneration has the effect of reducing the neutrino energy until it reaches a value at which it is not likely to interact. It can be understood as an *energy shift* to a fixed average energy that decreases as $\bar{\theta}$ increases but is independent of the primary neutrino energy. At $\bar{\theta} > 20°$ the energy is shifted down to energies below 10^{16} eV where there is hardly any difference between the considered models.

The corresponding τ-lepton P_{exit} energy distributions are shown in Fig. 12. Decreasing τ-lepton energy loss tends to narrow the distributions of E_τ, increasing the mode of the distribution in the region of small $\bar{\theta}$ and increasing the angle at which the plateau in E_τ starts. Decreasing the neutrino cross section tends to increase the angle at which the plateau ends and regeneration starts to dominate. This behavior indicates that with sufficient statistics, energy range, and range of emergence angles, the neutrino cross section and τ-lepton energy-loss-rate models could be constrained.

E. Exiting tau fluxes

So far we have treated the behavior of monoenergetic ν_τ's. In this section, we characterize the exiting flux of τ leptons

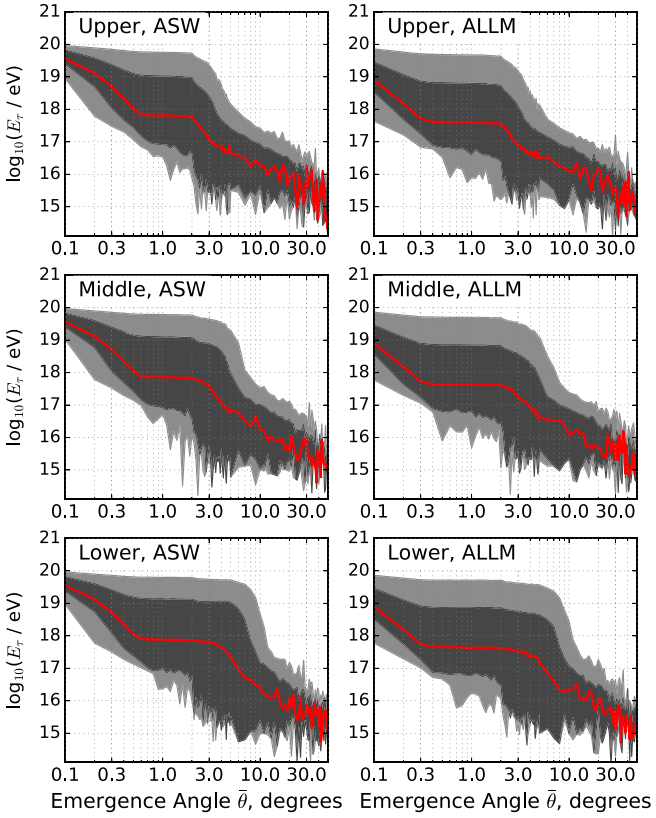

FIG. 12. The exiting τ lepton energies for various models corresponding to Fig. 11. On each panel, the cross-section model and energy-loss-rate models are labeled in the top right corner. The variance in exiting τ-lepton energies tends to increase as the cross section increases for trajectories that traverse mostly rock. The energy-loss model changes the range of emergence angles where the most probable energies plateau.

given a cosmogenic neutrino flux model. In Fig. 13 we show the Kotera 2010 [7] range of neutrino flux models along with the exiting τ lepton fluxes for emergence angles $\bar{\theta} = 1°$, 5°, and 10°. We have used the middle neutrino-nucleon cross-section curve and the ALLM τ-lepton energy-loss-rate model with a 4 km thick ice sheet. From Fig. 13 it is clear that τ leptons with the highest energy exit only at the smallest emergence angles. As the emergence angle increases, these τ leptons are suppressed with an enhancement of the τ lepton flux at $\sim 10^{17}$ eV and below. Note also that at the highest energies $10^{19} - 10^{20}$ eV, the τ lepton decay length is 490–4900 km, respectively, meaning that a high-altitude detector observing towards the horizon could potentially have a significantly improved sensitivity to these energies compared to a detector on the ground. Also note that at emergence angles of 10°, a ground-based detector is not likely to be able to observe a τ-lepton decay since the observables (Cherenkov optical or radio emission and secondary particles) are forward directed. Fluorescence emission could potentially be observed at these geometries but these detectors typically have low duty cycles.

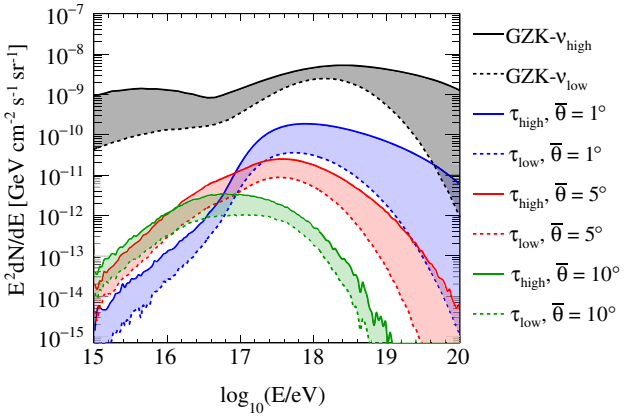

FIG. 13. The range of cosmogenic neutrino fluxes from Kotera 2010 [7] and the resulting flux of τ leptons for emergence angles $\bar{\theta} = 1°$, 5°, and 10° (see Fig. 2). The results use the middle neutrino-nucleon cross-section curve (Fig. 3), ALLM energy-loss rate (Fig. 4), and $D = 4$ km thick ice.

Finally we study how the different features contribute in concert for a given incident neutrino flux. For this purpose, we compare in Fig. 14 propagation through the Earth with a 4 km thick ice layer (0.92 g cm^{-3}) to propagation through regular rock (2.6 g cm^{-3}) for a neutrino flux centered in the previously discussed band [7]. We display the total exiting τ-lepton flux at several emergence angles and the fractions of the flux with a particular propagation history. As the number of ν_τ interactions in the Earth increases, the propagation history of the exiting τ leptons becomes increasingly complex and therefore we grouped the exiting τ leptons in the three following categories:

$N_{CC} = 1$: Exiting τ leptons resulting from a single ν_τ charged-current interaction (green lines).

$N_{NC} \geq 1$: Exiting τ leptons produced by a ν_τ that underwent at least one neutral-current interaction (red lines).

$N_D \geq 1$: Exiting τ leptons where at least one τ decay occurred in the chain of events leading to its production (black lines).

The $N_{NC} \geq 1$ and $N_D \geq 1$ fractions are not exclusive, but are chosen to illustrate when these two channels of ν_τ regeneration become important.

For very small emergence angles ($\bar{\theta} < 0.25°$), ν_τ regeneration is negligible, as can been seen in the top panel in Fig. 14. However, at $\bar{\theta} \simeq 1°$ the regeneration of ν_τ's becomes significant. In rock 20% (35%) of the exiting τ leptons exhibit in their propagation history one or more neutral-current interactions at $\bar{\theta} = 1°$ ($\bar{\theta} = 2°$). Because the density in ice is lower than in rock, the onset of regeneration in ice through neutral-current interactions happens at larger emergence angles. The fraction that underwent at least a single neutral-current interaction in ice is 8% at $\bar{\theta} = 1°$, but increases rapidly to 30% at $\bar{\theta} = 2°$. The regeneration through decaying τ leptons becomes a significant contribution only at larger emergence angles ($\bar{\theta} = 2°$), as can

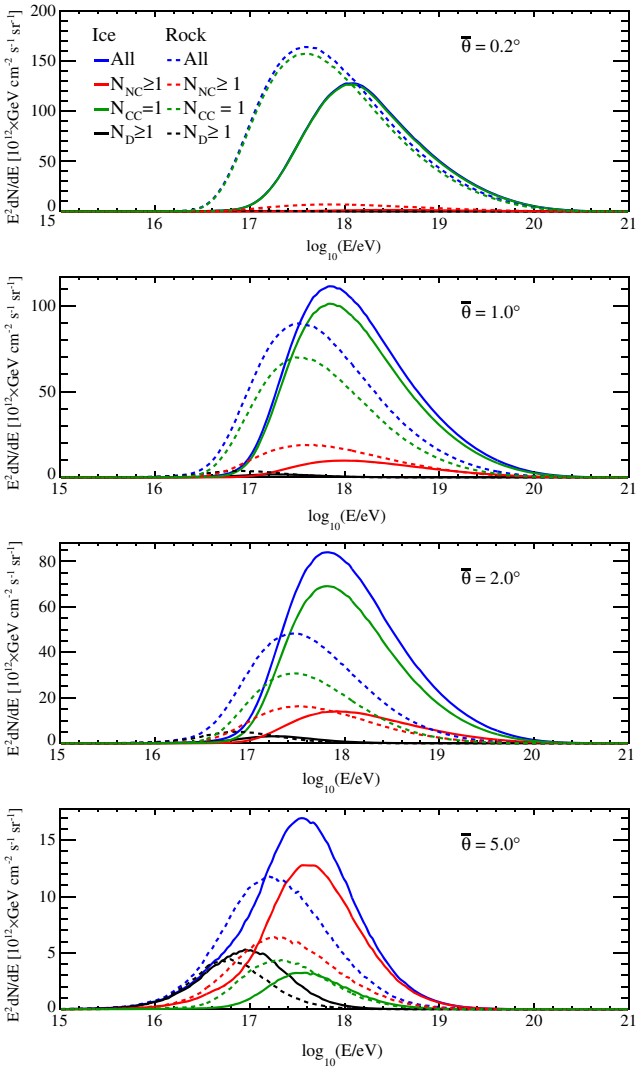

FIG. 14. The resulting flux of τ leptons for a cosmogenic neutrino flux in the middle of the flux ranges from Kotera 2010 [7] (gray band in Fig. 13). The different line colors indicate the interaction history that led to the exiting τ leptons (see text for more details). We show the effect of a 4 km thick ice layer (dashed lines) versus bare rock (solid lines) for four different emergence angles as indicated on the panels. These results are obtained using the middle neutrino-nucleon cross-section curve and ALLM energy-loss rate.

be observed from the lines labeled $N_D \geq 1$ in the bottom panel of Figure 14.

Because of lower energy losses and lower interaction probabilities, the total exiting τ-lepton flux peaks always at higher energies for the ice layer with respect to rock. Also, only at very small emergence angles ($\bar{\theta} \lesssim 0.3°$), the maximum energy flux (E^2dN/dE) of exiting τ leptons that propagated through rock exceeds that of a 4 km ice layer. At these angles, the integrated density of the ice provides less charged-current interactions than in rock. At larger angles, the ice layer is the more efficient medium to convert the neutrino flux into exiting τ leptons for neutrino energies $>3\times10^{18}$ eV because of the lower τ-lepton energy-loss rate (see Sec. IV C), giving a strong preference to experiments that would monitor ice or oceans for exiting τ leptons from ultrahigh-energy ν_τ's at small emergence angles.

V. DISCUSSION AND CONCLUSIONS

We have presented and characterized a ν_τ and τ-lepton propagation simulation that includes the effects of ocean or ice layer on Earth, as well as regeneration and variations on models of neutrino-nucleon interaction and τ-lepton energy-loss rate. The results of these simulations show that for ν_τ energies exceeding 3×10^{18} eV, the probability that a τ lepton exits the surface of the Earth into the atmosphere can be significantly boosted by the presence of a kilometer-scale thick layer of water or ice. The boost in the probability of exiting τ leptons is accompanied with a boost in energy and can be further enhanced depending on the neutrino-nucleon cross section and τ-lepton energy-loss-rate model. However, for ν_τ energies below 3×10^{18} eV, we have found that bare rock has an advantage due to the τ-lepton range being dominated by the decay lifetime, which is density independent, rather than energy loss, which is density dependent. In this study, we have also considered uncertainties consistent with the Standard Model and found significant variations.

Given the magnitude and variation of the exiting τ fluxes due to interaction uncertainties, they should be considered in the reported results of various experiments. It is possible that observatories on the ground or at altitude could have significantly different sensitivities depending on the choice of model even within Standard Model uncertainties. In particular, ground-based observatories are most sensitive to small emergence angles, where the dependence on the neutrino-nucleon cross section can be most pronounced. The potential benefit of observing at high altitude is to extend the range of emergence angles. Increasing the altitude of the detector enables observation of τ leptons exiting at larger emergence angles.

Observing at altitude could also be of interest for constraining the neutrino-nucleon cross section and τ-lepton energy-loss rates. With a sufficiently high neutrino event rate, the relative fraction of observations and energies as a function of emergence angle in the presence of a layer of water could be used to estimate the particle interaction parameters. An assessment of the sensitivity to these parameters will depend principally on detector altitude and on the existence of a water or ice layer, but ultimately on the detector characteristics as well as on the neutrino flux, which is currently unknown at these energies.

Consideration of the effects presented in this study should be of interest for future detectors proposing to constrain the UHE neutrino flux using the τ-lepton air shower channel. GRAND is proposing to place a large array of antennas on mountainous terrain on the ground,

which will present some altitude variations. CHANT, on the other hand, is proposing to observe these showers from stratospheric balloons or satellites, with the bulk of their sensitivity over oceans. Radio detection experiments at some altitude could also potentially observe τ leptons over various ice thicknesses and over the ocean.

ACKNOWLEDGMENTS

Part of this work was carried out at the Jet Propulsion Laboratory, California Institute of Technology, under a contract with the National Aeronautics and Space Administration. J. A.-M. and E. Z. thank María de Maetzu Unit of Excellence (Grant No. MDM-2016-0692), Ministerio de Economía (Grant No. FPA 2015-70420-C2-1-R), Xunta de Galicia (Grants No. GRC2013-024 and No. ED431C 2017/07), Feder Funds, Red Consolider Centro Nacional de Fisica de Partículas, Astropartículas y Nuclear (CPAN, FPA2015-69037-REDC) and Red Nacional Temática de Astropartículas (RENATA, Grant No. FPA2015-68783-REDT). W. C. thanks Grant No. 2015/15735-1, São Paulo Research Foundation (FAPESP). We thank N. Armesto and G. Parente for fruitful discussions on the neutrino cross section and τ-lepton energy-loss models.

[1] A. Aab *et al.* (Pierre Auger Collaboration), The Pierre Auger cosmic-ray observatory, Nucl. Instrum. Methods Phys. Res., Sect. A **798**, 172 (2015).
[2] T. Abu-Zayyad *et al.*, The surface detector array of the Telescope Array experiment, Nucl. Instrum. Methods Phys. Res., Sect. A **689**, 87 (2012).
[3] A. Aab *et al.* (Pierre Auger Collaboration), Combined fit of spectrum and composition data as measured by the Pierre Auger Observatory, J. Cosmol. Astropart. Phys. 04 (2017) 038.
[4] K. Greisen, The End of the Cosmic Ray Spectrum?, Phys. Rev. Lett. **16**, 748 (1966).
[5] G. T. Zatsepin and V. A. Kuzmin, Upper limit of the spectrum of cosmic rays, Pis'ma Zh. Eksp. Teor. Fiz. **4**, 114 (1966) [JETP Lett. **4**, 78 (1966)].
[6] V. S. Beresinsky and G. T. Zatsepin, Cosmic rays at ultra high energies (neutrino?), Phys. Lett. **28B**, 423 (1969).
[7] K. Kotera, D. Allard, and A. Olinto, Cosmogenic neutrinos: Parameter space and detectability from PeV to ZeV, J. Cosmol. Astropart. Phys. 10 (2010) 013, and references therein.
[8] D. Seckel and T. Stanev, Neutrinos: The Key to Ultrahigh Energy Cosmic Rays, Phys. Rev. Lett. **95**, 141101 (2005).
[9] A. Aab *et al.* (Pierre Auger Collaboration), Improved limit to the diffuse flux of ultrahigh energy neutrinos from the pierre auger observatory, Phys. Rev. D **91**, 092008 (2015).
[10] M. G. Aartsen *et al.*, Constraints on Ultrahigh-Energy Cosmic-Ray Sources from a Search for Neutrinos above 10 PeV with IceCube, Phys. Rev. Lett. **117**, 241101 (2016).
[11] T. H. Hankins, R. D. Ekers, and J. D. O'Sullivan, A search for lunar radio Čerenkov emission from high-energy neutrinos, Mon. Not. R. Astron. Soc. **283**, 1027 (1996).
[12] P. W. Gorham, C. L. Herbert, K. M. Liewer, C. J. Naudet, D. Saltzberg, and D. Williams, Experimental Limit on the Cosmic Diffuse Ultrahigh Energy Neutrino Flux, Phys. Rev. Lett. **93**, 041101 (2004).
[13] J. D. Bray, R. D. Ekers, P. Roberts, J. E. Reynolds, C. W. James, C. J. Phillips, R. J. Protheroe, R. A. McFadden, and M. G. Aartsen, A lunar radio experiment with the Parkes radio telescope for the LUNASKA project, Astropart. Phys. **65**, 22 (2015).
[14] P. W. Gorham *et al.* (ANITA Collaboration), Observational constraints on the ultrahigh energy cosmic neutrino flux from the second flight of the ANITA experiment, Phys. Rev. D **82**, 022004 (2010).
[15] M. G. Aartsen *et al.* (IceCube Collaboration), Observation of High-Energy Astrophysical Neutrinos in Three Years of IceCube Data, Phys. Rev. Lett. **113**, 101101 (2014).
[16] P. B. Denton, D. Marfatia, and T. J. Weiler, The galactic contribution to IceCube's astrophysical neutrino flux, J. Cosmol. Astropart. Phys. 08 (**2017**) 033.
[17] E. Roulet, G. Sigl, A. van Vliet, and S. Mollerach, PeV neutrinos from the propagation of ultra-high energy cosmic rays, J. Cosmol. Astropart. Phys. 01 (2013) 028.
[18] L. A. Anchordoqui *et al.*, Cosmic neutrino pevatrons: A brand new pathway to astronomy, astrophysics, and particle physics, J. High Energy Astrophysics **1**, 1 (2014), and references therein.
[19] L. A. Anchordoqui, M. M. Block, L. Durand, P. Ha, J. F. Soriano, and T. J. Weiler, Evidence for a break in the spectrum of astrophysical neutrinos, Phys. Rev. D **95**, 083009 (2017).
[20] H. Athar, H. Jezabek, and O. Yasuda, Effects of neutrino mixing on high-energy cosmic neutrino flux, Phys. Rev. D **62**, 103007 (2000).
[21] J. G. Learned and S. Pakvasa, Detecting ν_τ oscillations at PeV energies, Astropart. Phys. **3**, 267 (1995).
[22] D. Fargion, A. Aiello, and R. Conversano, Horizontal tau air showers from mountains in deep valley: Traces of UHECR neutrino tau, *Proceedings of the 26th International Cosmic Ray Conference, 1999, Salt Lake City, Utah, USA*, edited by D. Kieda, M. Salamon, and B. Dingus (International Union of Pure and Applied Physics (IUPAP), 1999), p. 396 [arXiv: astro-ph/9906450].
[23] A. Letessier-Selvon, Establishing the GZK cutoff with ultra high energy tau neutrinos, AIP Conf. Proc. **566**, 157 (2001).
[24] X. Bertou, P. Billoit, O. Deligny, C. Lachaud, and A. Letessier-Selvon, Tau neutrinos in the Auger Observatory: A new window to UHECR sources, Astropart. Phys. **17**, 183 (2002).

[25] J. L. Feng, P. Fisher, F. Wilczek, and T. M. Yu, Observability of Earth-Skimming Ultrahigh Energy Neutrinos, Phys. Rev. Lett. **88**, 161102 (2002).
[26] P. Gorham *et al.* (ANITA Collaboration), Characteristics of Four Upward-Pointing Cosmic-Ray-Like Events Observed with ANITA, Phys. Rev. Lett. **117**, 071101 (2016).
[27] Y. Asaoka and M. Sasaki, Cherenkov τ shower Earth-skimming method for PeV-EeV ν_τ observation with Ashra, Astropart. Phys. **41**, 7 (2013).
[28] A. Neronov, D. V. Semikoz, L. A. Anchordoqui, J. h. Adams, and A. V. Olinto, Sensitivity of a proposed space-based Cherenkov astrophysical-neutrino telescope, Phys. Rev. D **95**, 023004 (2017).
[29] O. Martineau-Huynh *et al.*, The Giant Radio Array for Neutrino Detection, Eur. Phys. J. Web Conf. **135**, 02001 (2017).
[30] E. Zas, Neutrino detection with inclined air showers, New J. Phys. **7**, 130 (2005).
[31] F. Halzen and D. Saltzberg, Tau Neutrino Appearance with a 1000 Megaparsec Baseline, Phys. Rev. Lett. **81**, 4305 (1998).
[32] O. Blanch Bigas, O. Deligny, K. Payet, and V. Van Elewyck, Ultrahigh energy τ neutrino flux regeneration while skimming the Earth, Phys. Rev. D **78**, 063002 (2008).
[33] S. Palomares-Ruiz, A. Irimia, and T. W. Weiler, Acceptances for space-based and ground-based fluorescence detectors, and inference of the neutrino-nucleon cross-section above 10^{19} eV, Phys. Rev. D **73**, 083003 (2006).
[34] F. Becattini and S. Bottai, Extreme energy τ neutrino propagation through the Earth, Astropart. Phys. **15**, 323 (2001).
[35] D. Fargion, Discovering ultra-high-energy neutrinos through horizontal and upward τ air showers: Evidence in terrestrial gamma flashes?, Astrophys. J. **570**, 909 (2002); D. Fargion, P. G. De Sanctis Lucentini, M. De Santis, and M. Grossi, Tau air showers from Earth, Astrophys. J. **613**, 1285 (2004).
[36] S. I. Dutta, M. H. Reno, and I. Sarcevic, Secondary neutrinos from τ neutrino interactions in the Earth, Phys. Rev. D **66**, 077302 (2002).
[37] J.-J. Tseng, T.-W. Yeh, H. Athar, M. A. Huang, F.-F. Lee, and G.-L. Lin, The energy spectrum of τ leptons induced by the high energy Earth-skimming neutrinos, Phys. Rev. D **68**, 063003 (2003).
[38] S. Bottai and S. Giurgola, UHE and EHE neutrino-induced taus inside the Earth, Astropart. Phys. **18**, 539 (2003).
[39] E. Bugaev, T. Montaruli, Y. Shlepin, and I. Sokalski, Propagation of τ neutrinos and τ leptons through the Earth and their detection in underwater/ice neutrino telescopes, Astropart. Phys. **21**, 491 (2004).
[40] S. Yoshida, R. Ishibashi, and H. Miyamoto, Propagation of EHE leptons in the Earth: Implications for their detection by the IceCube neutrino telescope, Phys. Rev. D **69**, 103004 (2004).
[41] C. Aramo, A. Insolia, A. Leonardi, G. Miele, L. Perrone, O. Pisanti, and D. V. Semikoz, Earth-skimming UHE τ neutrinos at the fluorescence detector of Pierre Auger Observatory, Astropart. Phys. **23**, 65 (2005).
[42] S. I. Dutta, Y. Huang, and M. H. Reno, Tau neutrino propagation and τ energy loss, Phys. Rev. D **72**, 013005 (2005).
[43] D. Gora, M. Roth, and A. Tamburro, A Monte Carlo approach to simulate up- and down-going neutrino showers including local topographic conditions, Astropart. Phys. **26**, 402 (2007).
[44] Y. S. Jeong, M. V. Luu, M. H. Reno, and I Sarcevic, Tau energy loss and ultrahigh energy skimming τ neutrinos, Phys. Rev. D **96**, 043003 (2017).
[45] K. Payet, Etude des neutrinos de Ultra-Haute Energie à l'Observatoire Pierre Auger, Ph. D. thesis, Univ. Joseph Fourier, Grenoble, France, 2010. Available at https://tel.archives-ouvertes.fr/tel-00451532v2.
[46] R. Gandhi, C. Quigg, M. H. Reno, and I. Sarcevic, Neutrino interactions at ultrahigh energies, Phys. Rev. D **58**, 093009 (1998).
[47] Parameters of the Preliminary Reference Earth Model are given by A. Dziewonski, Earth Structure, Global, in *The Encyclopedia of Solid Earth Geophysics*, edited by D. E. James (Van Nostrand Reinhold, New York, 1989), p. 331.
[48] S. Jadach, Z. Wąs, R. Decker, and J. H. Kühn, The τ decay library TAUOLA, version 2.4Comput. Phys. Commun. **76**, 361 (1993).
[49] N. Armesto, C. Merino, G. Parente, and E. Zas, Charged current neutrino cross section and τ energy loss at ultrahigh energies, Phys. Rev. D **77**, 013001 (2008), and references therein.
[50] A. Connolly, R. S. Thorne, and D. Waters, Calculation of high energy neutrino-nucleon cross sections and uncertainties using the Martin-Stirling-Thorne-Watt parton distribution functions and implications for future experiments, Phys. Rev. D **83**, 113009 (2011).
[51] F. Cornet, J. I. Illana, and M. Masip, TeV Strings and the Neutrino-Nucleon Cross Section at Ultrahigh Energies, Phys. Rev. Lett. **86**, 4235 (2001).
[52] A. Jain, P. Jain, D. W. McKay, and J. P. Ralston, Graviton enhanced UHE neutrino cross-sections and giant air showers, Int. J. Mod. Phys. A **17**, 533 (2002).
[53] M. M. Reynoso and O. A. Sampayo, Effects of large extra dimensions on cosmogenic neutrino fluxes, J. Phys. G **40**, 055202 (2013).
[54] H. L. Lai, J. Huston, S. Kuhlmann, J. Morfin, F. Olness, J. F. Owens, J. Pumplin, and W. K. Tung, Global QCD analysis of parton structure of the nucleon: CTEQ5 parton distributions, Eur. Phys. J. C **12**, 375 (2000).
[55] J. A. Castro Pena, G. Parente, and E. Zas, Measuring the BFKL pomeron in neutrino telescopes, Phys. Lett. B **500**, 125 (2001).
[56] H. Abramowicz and A. Levy, The ALLM parameterization of $\sigma_{\rm tot}(\gamma^* p)$: An update, arXiv:hep-ph/9712415.
[57] N. Armesto, C. Salgado, and U. A. Wiedemann, Relating High-Energy Lepton-Hadron, Proton-Nucleus, and Nucleus-Nucleus Collisions through Geometric Scaling, Phys. Rev. Lett. **94**, 022002 (2005).